Thermal Conduction from Coil: Assessment of Effects and Comparison to Simulation

Sukhoon Oh[1], Giuseppe Carluccio[2], and Christopher M Collins[1]

[1]*Center for NMR Research, Radiology, The Pennsylvania State University, Hershey, PA, United States,* [2]*Electrical and Computer Engineering, University of Illinois at Chicago, Chicago, IL, United States*

Introduction: It is well known that the RF energy used in MRI can cause heating of tissues. It is generally assumed that the main mechanism of heating is through magnetic induction, though other mechanisms are possible, especially when the subject is very near the coil and near the coil capacitors. In some circumstances, conservative electric fields can cause significant heating [1], and in cases where the coil is both driven with a high enough duty cycle as to become hot and placed very near the subject, thermal conduction could become a mechanism for heat transfer to the subject. Heating of the subject due to thermal conduction from the coil would not be represented in estimates of SAR based on measurements of loaded and unloaded Q or based on field simulations. As a result, thermal conduction can be a source of error between temperature simulations and measurements. In this study, we evaluate heating of a phantom adjacent a surface coil driven with a high duty cycle and placed two different distances from the phantom. We performed field calculations, temperature simulations, MR-based PRF temperature mapping, and acquired infrared (IR) thermal images for each case.

Methods: The surface coil shown in Figure 1a was driven with 42.5W of CW RF power (assessed with directional coupler and power sensor and accounting for cable loss) for two minutes when placed with its 6mm casing adjacent a gel phantom (D=0mm) and with an 8mm air space between the casing and the phantom (D=8mm). IR images of the coil (not shown) indicate much greater temperatures near the capacitors than elsewhere. In Figure 1c (sagittal views of phantom), we conceptually show the thermal conduction from the regions of the capacitors in red, and from the conductive elements in green. In both cases, the coil (diameter=80mm) was beneath the agar-gel phantom (σ=2.97S/m, ε_r=74.15, ρ=1021 kg/m^3, w×d×h=88×154×68mm^3, Figure 1b). The surface coil was connected to a separate RF amplifier with frequency synthesizer at 165.5MHz. We acquired three axial temperature maps on planes intersecting the two capacitors and on the plane through center of the phantom and coil using the proton resonance frequency shift method on a Siemens 3T system using an extremity volume coil for imaging [2, 3]. We also acquired turbo-spin-echo images of the phantom to build a voxel model for SAR simulations using XFdtd (Remcom, Inc., USA). The simulated SAR was then used for temperature simulations [4]. We measured the Q-ratio of the heating coil as 0.05, indicating 95% of the RF power will be dissipated in the phantom with D=0mm. We simulated temperature changes using the simulated SAR and measured Q-ratio, and then compared with experimentally acquired temperature maps at different slice positions (Table 1). We repeated the above procedure for both D=0mm and D=8mm. Immediately after identical protocols outside the magnet, IR thermal images (E60bk, FLIR system, Inc., USA) were acquired of the Teflon coil casing and the bottom of the phantom.

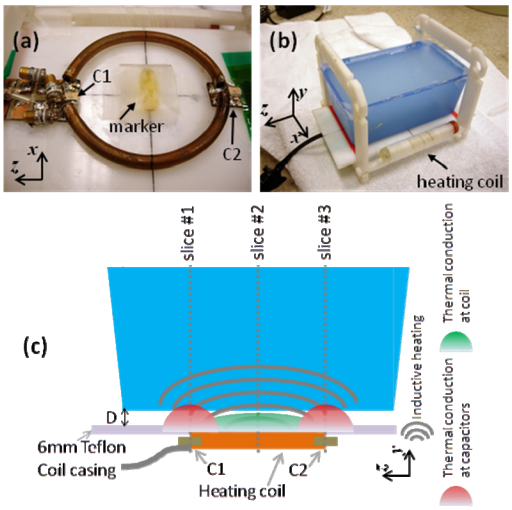

Figure 1. Experimental setup: photographs of the heating coil (a) and phantom (b) and schematic diagram. In (c), "D" indicates distance between Teflon plate and bottom of phantom. MR-based PRF thermography was performed on slices 1, 2, and 3.

Results and Discussion: In Figure 2, we show the measured IR temperature maps of the coil casing and adjacent surface of the phantom after 2 minutes of heating with D=0mm and D=8mm. The maximum ΔT at C1 and C2 were 5.9 and 5.3 °C when D=0mm. The maximum ΔT at C1 and C2 is much higher (11.0 and 8.4 °C) when D=8mm. Conversely, the surface of the phantom is notably cooler when D=8mm. This indicates that when the coil is very near the phantom (D=0mm), heat can be conducted from the high-temperature regions near the capacitors to the phantom effectively, though it is clear from the heating pattern that inductive heating is still the dominant mechanism for temperature increase in the phantom. However, if the coil is a little further from the phantom (D=8mm), the thermal energy remains in the coil and the temperature of the coil capacitors is greater. Interestingly, in this case (D=8mm) the conductive elements of the coil are slightly cooler than before (D=0mm), indicating that in these regions heat may actually be conducted from the phantom (which is hotter in the corresponding regions) to the coil when D=0mm. Simulated temperature distributions based on SAR but not considering thermal conduction from the coil (not shown) are in notably better agreement with measured (both MR-based and IR-based) when D=8mm than when D=0mm (Figure 3). Table 1 summarizes this in minimal space with comparison of maximum temperatures in simulation and MR-based measurements in simulation and experiment for both D=0mm and D=8mm.

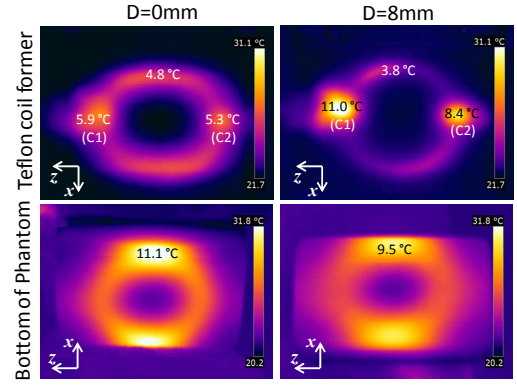

Figure 2. IR thermal images of the Teflon plate and bottom surface of the phantom immediately after 2 minutes of 42.5 W RF power delivered to the coil with no air space between coil casing and phantom (D=0mm) and with an 8mm air space (D=8mm).

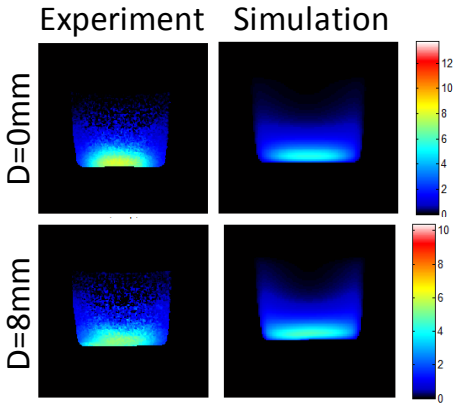

Figure 3. MR-based and simulation-based maps of temperature increase on slice 1 ad D=0mm and D=8mm.

Table 1. Maximum temperature increase in temperature simulations and experiments at each slice position and at each distance D, and their difference in percentage.
(Exp.= experimental, Sim.= simulation, Diff=difference)

	D=0mm			D=8 mm		
	Exp.	Sim.	Diff.	Exp.	Sim.	Diff.
Slice #1	8.35°	5.76°	31.0%	5.51°	4.82°	12.5%
Slice #2	13.69°	11.97°	12.6%	10.40°	10.37°	0.3%
Slice #3	8.77°	6.23°	29.0%	6.53°	5.10°	21.9%

Acknowledgment: This study was funded from NIH R01 EB000454 and NIH R01 EB006563.

References:

1. Park *et al*., JMR 2010;202:72-77
2. Oh *et al.*, MRM 2010;63:218-223
3. Oh *et al.*, ISMRM 2011 p 3863
4. Collins *et al.*, JMRI 2004;19:650-656